

Comparison of Analog Continuum Correlators for Remote Sensing and Radio Astronomy

Olli Koistinen, Janne Lahtinen, and Martti T. Hallikainen, *Fellow, IEEE*

Abstract—Two different designs of analog correlators for radiometry are compared in this paper. A continuum correlator based on a microwave nonlinear device is a simple and inexpensive way to detect wide-band polarized signals. Analysis and extensive measurements including linearity, dynamic range, amplitude response, phase balance, and stability are presented, and the suitability of the designs for microwave radiometry is discussed. Both correlators showed nearly ideal performance. A novel method for determining the correlator degradation factor is applied.

Index Terms—Analog correlator, complex cross-correlation, polarimetric radiometry, radio astronomy, remote sensing.

I. INTRODUCTION

THE knowledge of the polarization state of a measured signal gives valuable information on the physics of the measured object both in remote sensing and in radio astronomy. The polarization state can be expressed with four parameters known as the Stokes parameters or vector. Since many measurements do not require spectral information, a simple and inexpensive analog correlator may be used to measure the Stokes parameters. Various analog correlator designs, such as a wideband correlator for astronomy and an electro-optic correlator (see [1], [2]), have been presented in the literature.

The operation principle of a receiver or radiometer capable of measuring the polarization state can be coherent or incoherent [3]. Both receivers described here are based on the coherent approach, which applies the complex cross-correlation of two orthogonal polarizations. The principle of the coherent two-channel polarimetric receiver is similar to an interferometer baseline with the baseline length set to zero. The complex cross-correlator consists of two identical correlator subunits that are fed with in-phase and quadrature signals. Non-linear semiconductor devices such as mixers or multipliers may be used as the active elements of the correlators.

Metsähovi radio observatory makes solar observations at 22, 37, and 90 GHz. A mixer-based correlator was designed for the polarization sensitive receiver at 37 GHz. The large dynamic range requirements of solar measurements have to be considered in the design of such a receiver.

Manuscript received December 10, 1999; revised December 26, 2001. This work was supported in part by the National Technology Agency (Tekes Contract 40206/98), Graduate School in Electronics, Telecommunications and Automation (GETA), Foundation of Technology, and the Vilho, Yrjö, and Kalle Väisälä Foundation.

O. Koistinen is with the Metsähovi Radio Observatory, Helsinki University of Technology, Espoo, Finland.

J. Lahtinen and M. T. Hallikainen are with the Laboratory of Space Technology, Helsinki University of Technology, Espoo, Finland.

Publisher Item Identifier S 0018-9456(02)02914-5.

An analog multiplier-based correlator unit was constructed for the Helsinki University of Technology (HUT) 36.5 GHz polarimetric radiometer [4]. The HUT polarimetric radiometer is a part of the Helsinki University of Technology radiometer (HUTRAD) multifrequency airborne radiometer system for remote sensing of the Earth's surface [5].

In this paper, two different analog correlator approaches are studied. Applying the same measurements allows comparison of the applicability of the designs to the different system requirements. The HUT polarimetric radiometer requires good long term stability due to the long calibration interval at airborne use, while the stability requirement for the solar receiver is not as vital due to the considerably shorter calibration cycle. On the other hand, the solar receiver requires wide bandwidth to maintain high sensitivity at high brightness temperatures. Measurement of the key parameters of the devices was very accurate while requiring only standard equipment. The methods used to make the extensive measurements of the study included a novel method for determining the degradation factor of the correlator.

This paper is set out in the following way: Section II characterizes the system requirements and the theoretical background for the measurements of the correlators. Section III presents the correlator designs. Section IV describes the measurements of input match, dynamic range, response and stability. The results are concluded and discussed in Section V.

II. DESIGN CONSIDERATIONS

The theoretical limit for the sensitivity of the correlation channel is determined by the rms value of the correlator output signal fluctuation in the absence of correlated input signals. The sensitivity of a correlator radiometer can be obtained by applying the signal-to-noise ratio of a single baseline in an aperture synthesis receiver [6]. Assuming a uniform distribution for the brightness temperature (T_B) and rectangular amplitude response, flat phase response, and an ideal integrator of the receiver, the sensitivity of the correlator output becomes

$$\Delta T_{\min} = K \sqrt{\frac{(T_{A,m} + T_{S,m})(T_{A,n} + T_{S,n}) + T_{A,m}T_{A,n}}{2B\tau}} \quad (1)$$

where $T_{A,m}$ and $T_{A,n}$ are the polarized target-generated antenna temperatures of the two different channels (e.g., vertical and horizontal), B is the receiver noise bandwidth [7] and τ is the integration time. The receiver system temperatures for the different channels ($T_{S,m}$ and $T_{S,n}$) consist of receiver noise temperatures and the antenna temperatures generated by the unpolarized targets. The value for K is 1 for total power receivers and

2 for Dicke-type receivers. It has to be noted that polarimetric brightness temperature information is expressed with the third (T_3) and fourth (T_4) Stokes parameters, which are computed from $T_3 = 2 \times \text{Re}\{\langle E_V E_H^* \rangle\}$ and $T_4 = 2 \times \text{Im}\{\langle E_V E_H^* \rangle\}$. The sensitivities of these measurements are thus twice that predicted in (1). The E_V and E_H stand for the vertically and horizontally polarized electric fields; the asterisk * denotes the complex conjugate.

In many cases, the degree of polarization of the target is small, i.e., $T_A \ll T_S$. This applies, for example, to most remote sensing targets and for the quiet Sun. Equation (1) can thus be simplified to

$$\Delta T_{\min} \approx K \sqrt{\frac{T_{S,m} T_{S,n}}{2B\tau}}. \quad (2)$$

At the other extreme, $T_A \gg T_S$. This applies, for example, to the observation of solar radio bursts. In this case, (1) simplifies to

$$\Delta T_{\min} \approx K \sqrt{\frac{T_{A,m} T_{A,n}}{B\tau}}. \quad (3)$$

Due to the correlator nonidealities, the correlator channel practical sensitivities are worse than those obtained from (1)–(3). The parameters that degrade the correlator sensitivity are the input matching, amplitude response, phase response, delay differences between the input signals, and correlator internal noise. The sensitivity degradation due to the response nonidealities is expressed using a degradation factor D [8]

$$D = \frac{\left| \int_0^\infty G(f) \cos[\delta(f)] df \right|}{\left[\beta \cdot \int_0^\infty G^2(f) df \right]^{1/2}} \quad (4)$$

where $G(f)$ is the correlator amplitude response, $\delta(f)$ is the correlator phase response and β is the passband bandwidth. Note that the noise bandwidth B equals the passband bandwidth β only if the passband is rectangular. For analog correlators, the value of D is typically ≥ 0.9 [2]. Amplitude and phase errors caused by nonidealities in the receiver RF channels are beyond the scope of this presentation and are not considered here. Differences in signal delays inside the correlator are minimized in the design and can be neglected.

The individual design specifications for input matching, phase variation, amplitude flatness, and ripple values were chosen in order to keep the degradation factor better than 0.97 for each parameter. Assuming that the parameters are independent, this gives a worst-case overall degradation factor $(1 - 4 \times 0.03) = 0.88$. However, the individual parameters cannot be dealt with separately from each other and were only used as a starting point for the design. The passbands of the correlators were specified to cover the Metsähovi and Laboratory of Space Technology receiver passbands, respectively. The reflections in inputs cause errors in correlator amplitude and phase responses, which decrease D . A maximum return loss figure was obtained by applying worst-case analysis for its influence on D . The amplitude ripple figure corresponds to sine type variations. A linear slope was used in the amplitude slope calculation. The specifications for the individual parameters giving $D \geq 0.97$ for the mixer and multiplier correlators

TABLE I
SPECIFICATIONS FOR THE CORRELATORS

	Mixer correlator	Multiplier correlator
Passband (MHz)	100 – 1000	90 – 520
Amplitude slope, linear (dB)	< 4.0	
Amplitude ripple, p-p (dB)	< 3.2	
Mean of phase variations (deg)	< 14	
Input matching	< -9.5 dB	
Degradation factor D	0.89	

are presented in Table I. The mixer correlator is used for the Metsähovi polarimetric receiver, which operates in total power mode and has double side-band vertical and horizontal channel noise temperatures of 420 K and 425 K, respectively. The multiplier correlator is used for the Laboratory of Space Technology polarimetric receiver, which operates in Dicke mode and has single side-band vertical and horizontal channel noise temperatures of 1500 K and 1200 K respectively. For the mixer correlator, the sensitivities calculated with (2)–(3) are $\Delta T_{\min} = 0.27$ K for the silent Sun (low polarized flux) and $\Delta T_{\min} = 36.8$ K for a solar radio burst (high polarized flux) with an integration time $\tau = 0.5$ s. The calculated sensitivity for the multiplier correlator using (2) is $\Delta T_{\min} = 0.16$ K with $\tau = 0.5$ s. The seemingly higher ΔT_{\min} for the mixer correlator is due to the high microwave emission from the sun that adds to the system noise temperature.

III. CORRELATOR DESIGNS

A. General Design

Two different continuum analog correlators were constructed for microwave receivers operating at Ka band. Both correlators are based on the complex correlator design where two identical correlator subunits are used. The signals from the two receiver channels are fed in-phase and quadrature shifted to the subunits. As a result, the subunits are sensitive to linear and circular polarizations while the unpolarized signal cancels out. The differences between the receiver channels and the input circuitry for the correlator active units are minimized to avoid signal variations due to attenuation, dispersion, and delay deviations in the components. The block diagrams of the complex correlators are presented in Fig. 1.

The noise level of the post-correlator components is very low and can be neglected. The RF bands of the two receivers are somewhat different, leading to different input match realizations for the correlators and affecting the choice of the active correlator element. The stability requirement leads also to differences in the designs. The differences are presented in the following.

B. Detailed Designs

1) *Mixer Correlator for Solar Radio Astronomy*: The mixer correlator detects basically zero polarization from the silent sun whereas a radio burst can be nearly 100 % circularly polarized with a total intensity rise of up to 20 dB at 37 GHz. The brightness temperature of the silent Sun is 7800 K. The integration time is 10 ms for the mapping of the Sun, while for tracking the active regions the integration time is adjusted to 0.2 ms.

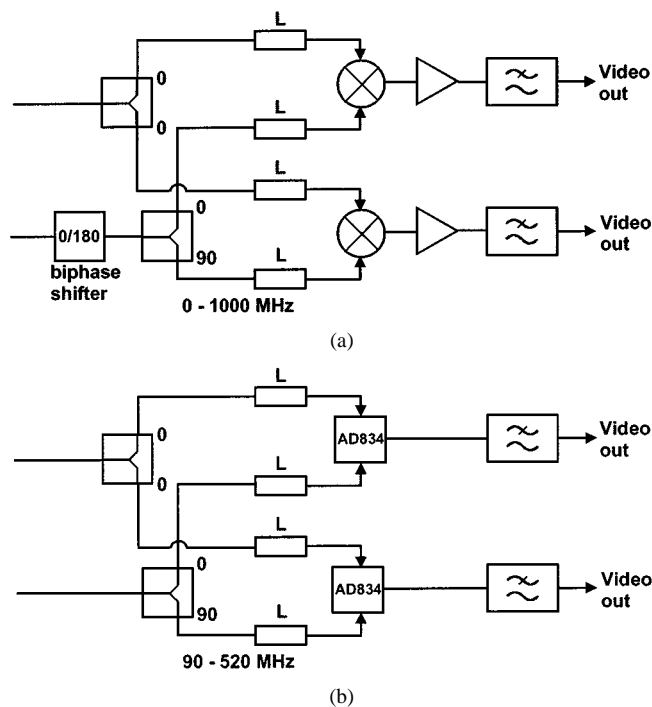


Fig. 1. General block diagram of a complex correlator. The complex correlator consists of two identical correlator subunits and a quadrature phase shifter; (a) mixer correlator; (b) multiplier correlator.

A biphaser is used at one input port of the mixer correlator to remove the uncorrelated bias term from the signal. As the phase of either input of the correlator changes by 180° the sign of the correlated output signal changes while the uncorrelated signal remains the same. By subtracting a cycle of phase changes, the uncorrelated signal cancels out. Removing the uncorrelated fluctuations also enhances considerably the dynamic range and the stability of the mixer correlator.

The active elements for the mixer correlator are commercially available double-balanced mixers with a nominal frequency coverage of 5–1500 MHz (Mini-Circuits RMS-5). The input ports can be matched to line impedance with RF attenuators. These attenuators provide a wide bandwidth match at the input ports of the correlator. Indeed, the S_{11} of the LO port of the unmatched correlator element is -4 dB which is unacceptably high, but very flat up to 1400 MHz. The S_{11} at the RF port instead is -9 dB at lower frequencies, but increases rapidly at 1 GHz and thus decreases the performance of the correlator above 1 GHz. Chip attenuators of 9 dB and 12 dB are added at the LO and RF ports, respectively, to compensate for the reflection losses in the LO and RF ports. This provides equal input power levels at both ports of the mixer elements. A better than 20 dB return loss at both ports of the correlators is achieved with these values over a wide bandwidth. The introduced attenuation can be easily compensated without decreasing the linearity of the receiver RF components. As the correlator is placed at the end of the receiver chain, the lossy match does not degrade the signal-to-noise ratio.

The LO and RF signals applied to the correlator active element have to be low to ensure small signal conditions for the mixer diodes over the whole input power range. This leads to

low video signals which request in counter part high video gain (of the order of 70 dB) to reach sufficient signal levels for A/D conversion. The high gain tends to degrade the stability by amplifying the thermal fluctuations of the signal in the correlator active element. The shift rate of the biphaser has to be at least 100 Hz to remove these drifts.

2) *Multiplier Correlator for Polarimetric Remote Sensing*: The multiplier correlator detects the polarized component of brightness temperatures emitted by remote sensing targets. Few targets have a polarized component and for natural objects the degree of polarization is normally only a few percent. The amplitude of the detected polarized signal is thus typically a few Kelvins. The Laboratory of Space Technology radiometer system is installed onboard a research aircraft. A 0.5 s integration time is determined by the aircraft ground speed (50 m/s) and the footprint size of the antenna (50 m to the flight direction).

The operation principle of the multiplier correlator is similar to that of the mixer correlator. The complex cross-correlator consists of two correlating subunits and a wide-band 90° hybrid. The correlating subunits are based on commercially available Gilbert cell analog multipliers (Analog Devices AD834) with a nominal frequency coverage of 0–500 MHz. The structure of the subunits is symmetric for both input channels. In order to maximize the bandwidth, the transmission line lengths are kept to a minimum on the circuit board and surface mount components are used in the correlator input. Resistive input matching on the board is used for the multiplier inputs.

IV. MEASUREMENTS

As the complex correlator consists of two identical correlator subunits and a quadrature phase shifter, the characteristics can be determined by measuring only one sub-unit.

A. Input Match

Poor match at the input ports of the correlator degrades the correlator quality by introducing standing waves that cause fluctuations to the signal amplitude and phase response. The input reflection coefficients of the correlators were measured with a network analyzer under small signal conditions.

The measured input reflection coefficients of the mixer correlator obtained after inserting the matching attenuators are presented in Fig. 2. The final input matches at the RF and LO ports are almost identical. However, due to the variation of the reflection at the RF port of the active device, the amplitude and phase responses degrade above 1 GHz.

The measured reflection coefficients for the multiplier correlator inputs are also presented in Fig. 2. The input ports are well matched over the intended passband; the maximum reflection coefficient is -17 dB. The reflection coefficient is -22 dB up to about 450 MHz, but at higher frequencies the matching decreases rapidly. The current input match would enable the use of the multiplier correlator up to about 700 MHz. The use of the correlator at even higher frequencies would require wider-band match.

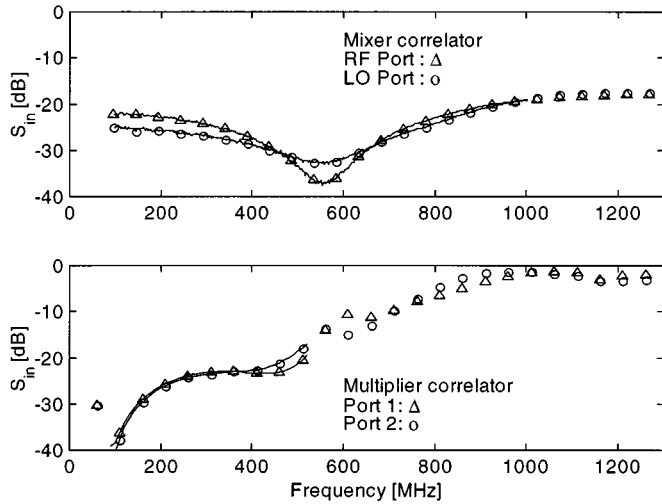


Fig. 2. Measured reflection coefficients at the input ports of the mixer correlator (above) and the multiplier correlator (below). The passbands are indicated with solid lines.

B. Linearity and Dynamic Range

The dynamic ranges of the mixer and multiplier correlators were measured with a signal source at 300 MHz. An in-phase signal was fed into the input ports of the correlators and the output voltage levels were measured with a multimeter.

The measured dynamic ranges of the correlators are shown in Fig. 3. The peak-to-peak value for a sine signal is $2\sqrt{2} \times \text{rms}$ value while for white noise the factor is 6 (99.7% confidence or the 3σ limit). To avoid compression of the noise signal peaks, the maximum linear input level for noise has to be set 3 dB lower than that obtained with a sine signal. The low end of the power range is limited also by the RF noise of the measurement equipment and the signal sources. A 0.5 s integration time was used in the measurement.

The dynamic range of the mixer correlator is limited by the nonquadratic behavior of the mixer at high input power levels ($P_i > -20$ dBm) when the mixer diodes may no longer be considered to operate under small signal conditions. For a full range input for the A/D converter, the video gain of the correlator output amplifier has to be increased as the RF input power level is lowered in order to get a linear response of the mixer. A nonlinearity of max. 0.2 dB is detected with $P_i < -20$ dBm over the measured input power range. On the other hand, at very low input power levels, the thermal fluctuations of the signal in the correlator elements may be significant and affect the sensitivity of the correlator. The dynamic range of the mixer correlator is determined by the Allan variance measurement [9] scaled to the measured maximum linear input power level. The Allan variance gives a good estimate of the dynamic range as well as the stability of the device. Measurements of the Allan variance are presented in detail in Section IV-D.

The multiplier correlator is based on a balanced differential circuit. Due to the topology, the dynamic range is large. The 1 dB compression point of the device is +13 dBm and the maximum linear output is detected with $P_i = +9$ dBm. A maximum nonlinearity of 0.2 dB p-p between -32 dBm and +9 dBm is probably caused by the measurement procedure,

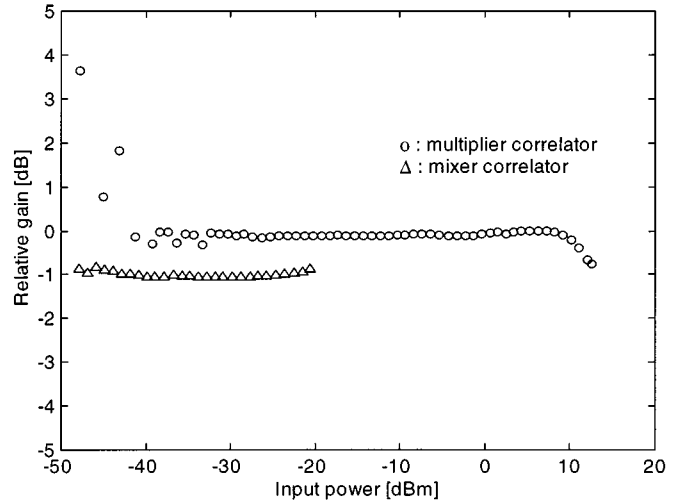


Fig. 3. Measured linearities of the correlators. The measurements are made with a 300 MHz sine signal.

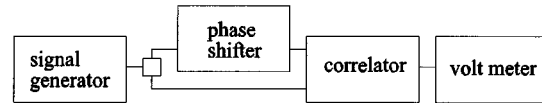


Fig. 4. Measurement setup for amplitude and phase responses of the correlators.

which uses a set of attenuators to increase the dynamic range of the power meter that was used to measure P_i . The ripple at the low end, $P_i = -41$ – -33 dBm is generated by quantization error at the correlator output voltage measurement. The low end of the measurement is limited by the thermal fluctuations to $P_i = -41$ dBm. The dynamic range of the multiplier correlator is thus at least 47 dBm for noise signals. As the calibration sequence for the multiplier correlator is considerably longer than the white noise limit, the dynamic range cannot be determined by the Allan variance measurement.

C. Amplitude and Phase Response

The measurement setup for the amplitude and phase response of the correlators is shown in Fig. 4. In the measurement setup, the signal from the synthesized signal source is divided and the electrical length of one branch is tuned to find the maximum correlation. A mechanical phase shifter is applied and the phase response is calculated from the offset of the phase shifter. The in-phase output voltage value is used for the amplitude response calculation. The measured amplitude and phase responses of the correlators are presented in Fig. 5. These values are applied to (4) to calculate the correlator degradation factor. The input power levels for the measurements were +5.5 dBm and -14 dBm for the multiplier correlator and the mixer correlator, respectively.

The amplitude variation of the mixer correlator is less than 1 dB over a 100–1000 MHz band while the phase variation is smaller than 17° p-p or 3° mean. The reference point 0° corresponds to the phase shifter physical length, which gives the optimum degradation factor D . Although the amplitude response lies within 3 dB up to 1250 MHz, the phase variation becomes

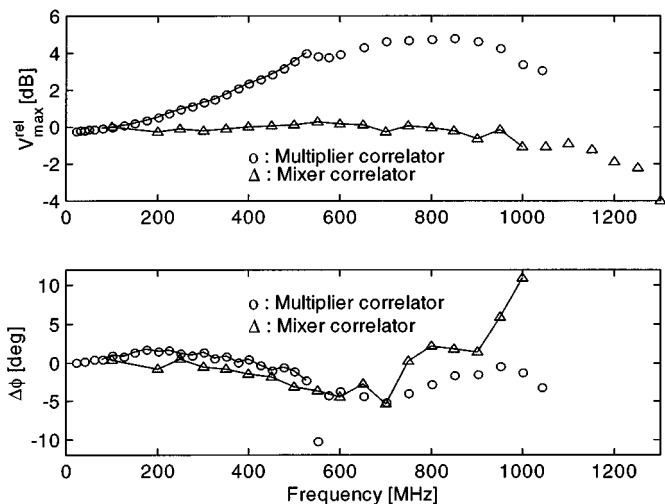


Fig. 5. Measured amplitude responses (above) and phase responses (below) of the mixer and multiplier correlators. The passbands are indicated with solid lines.

large above 1000 MHz. This is mainly due to the poor return loss at the RF input of the mixer element.

The amplitude response of the multiplier correlator increases with frequency, and the response slope at the 90–520 MHz frequency range is 3.9 dB. On the other hand, the phase variations over the specified frequency band are small, 4° p-p or 1° mean. At input power levels above $P_{\text{in}} = +5$ dBm, the phase response of the multiplier correlator changes as a function of input power. This anomaly was measured at 300 MHz when a slope of about $1.3^\circ/\text{dB}$ was detected, the phase shift being 90° between the input channels. A slope of about $0.4^\circ/\text{dB}$ was detected at a phase shift of 0° . The maximum error was at about $P_{\text{in}} = +11$ dBm; at higher input power levels the anomaly seems to decrease. The power variations in the correlator input are less than 1 dB ($P_{\text{in}} = +5.1$ dBm to $+5.7$ dBm) when used as a part of a remote sensing polarimetric radiometer; thus, the influence of this phenomenon is small. However, in applications where the input power variations are large the dynamic range of the multiplier correlator has to be reduced by an additional 4 dB from that determined in Section IV-B. The phase response anomaly described above was not detected in the dynamic range of the mixer correlator.

The measured phase and amplitude response nonidealities cause a 0.3% degradation to the mixer correlator sensitivity ($D = 0.9968$) and 3.5% degradation to the multiplier correlator sensitivity ($D = 0.965$). Due to the amplitude variations, the mixer correlator noise bandwidth decreases only minimally to 897 MHz (instead of 900 MHz), the multiplier correlator bandwidth somewhat more to 403 MHz (instead of 430 MHz).

D. Stability

The thermally induced fluctuations at the correlator output may be significant compared to the measured signal. The stabilities of the correlators were measured in time domain by sampling the output of the correlator with a stable test signal.

The Allan variance [9], [10] of a series of discrete data can be calculated by forming M samples $R_n(K)$ of variable width

from N samples of the original data x where K represents the duration of one sample

$$R_n(K) = \frac{1}{K} \sum_{l=1}^K x_{nK+l} \quad n = 0, 1, \dots, M \quad M = \frac{N}{K} - 1. \quad (5)$$

The Allan variance is the weighted sum of the difference of successive samples

$$\sigma_A^2(K) = \frac{1}{2} \frac{1}{N-1} \sum_{n=1}^{N-1} [R_{n+1}(K) - R_n(K)]^2. \quad (6)$$

By plotting the results, different types of noise can be detected. Assuming a simple power law relation for the noise spectral density, the dominant noise type is detected from the slope of the curve on a log–log plot. A slope of -1 is produced by white noise, 0 by flicker noise and a rising slope is produced by drift. A slope of $+1$ stands for linear drift. The corner for white noise corresponds to the longest integration time that improves the sensitivity.

The Allan variances for the correlators were calculated relative to the maximum signal levels. The experimental values are shown in Fig. 6. Here, $N = 24447$ samples and $N = 200000$ samples were used for the multiplier correlator and the mixer correlator, respectively. Two important conclusions are obvious for the mixer correlator. The results show that the phase shifter for the elimination of the noncorrelating bias stabilizes the correlator and the white noise corner is still not detectable with 30 s sample times. Second, the phase shift frequency has to be higher than 100 Hz to keep the measurement in the region where white noise dominates. This can be seen from the deviation between the measurements with the phase shifter on and off.

The multiplier correlator shows good stability with a noise corner of 10 s and superior noise levels compared to the mixer correlator. The large difference in the noise levels is due to the inherent architecture of the correlating elements. The multiplier correlator utilizes a differential Gilbert cell layout with internal thermal compensation, while the mixer correlator is based on a double balanced mixer without thermal compensation elements. A Gilbert cell produces linear output for high input levels as was seen in Section IV-B, whereas the balanced mixer has to operate at low input levels, therefore needing high video gain, which reduces the S/N ratio. The relative noise level of the multiplier correlator is 10 dB lower than that of the mixer correlator. Although the Allan variance figure increases at longer integration times it does not exceed high levels: At $\tau = 1000$ s integration time the Allan variance is -53 dB indicating that the drift of the multiplier correlator is small. This is a vital characteristic as the calibration period of Laboratory of Space Technology polarimetric radiometer is typically 2–4 h. Because the calibration period is considerably longer than the optimal level detected by the Allan variance measurement, the standard deviation of the output signal gives a better estimate for the dynamic range. The standard deviation presented in Fig. 6 agrees with the measured value of the dynamic range in Fig. 3.

The multiplier correlator produced a ± 0.001 mV noise level with a 0.5 s integration time. The maximum linear output signal

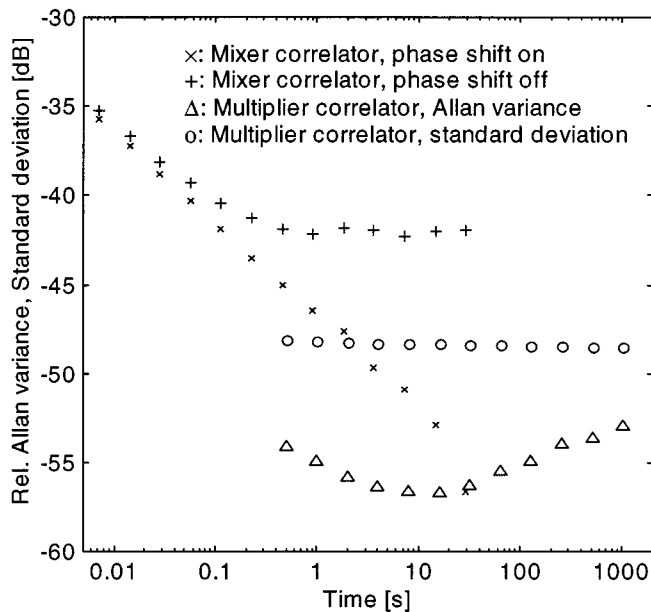


Fig. 6. Measured stability characteristics of the correlators.

level is 115 mV at 300 MHz and $P_i = +6$ dBm. The mixer correlator introduced a ± 0.2 mV noise level with a 0.5 s integration time. The maximum linear output signal level for the mixer correlator is 2.4 V.

E. Summary of Measurements

The measured overall characteristics of the mixer and multiplier correlators are presented in Table II. For the mixer correlator the amplitude and phase responses at the specified frequency range are flat, lying well within the specifications. This gives a nearly ideal degradation factor D of 0.9968. Although the amplitude response of the multiplier correlator is not as flat as that of the mixer correlator, it nevertheless lies within the specifications. On the other hand, the phase response is very flat: the mean of the variations from the reference point is only 1.0° . The resulting degradation factor is also close to ideal: 0.965. The nearly ideal degradation factors suggest that the sensitivities of both correlators are close to the values determined in Section II.

The Allan variance figure of the multiplier correlator is low also for very long integration times. The drifting of the correlator response is thus small which is a vital characteristic when calibration period is long. The mixer correlator equipped with a phase shifter is very stable showing no drift at 30 s sampling times that suggests that even longer integration times can still be used without degrading the sensitivity.

The input match for both correlators is significantly better than the specified value -9.5 dB. The mismatch was thus not taken into account in the calculation of the degradation factor values.

Price *et al.* [2] have measured the degradation factor with a different method that also includes the noise of the correlator video electronics. This noise component, however, can be neglected if the electronics is properly designed and the method should give the same values for the degradation factor as the one described here. A reference measurement for the mixer correlator with the setup presented in [2] produced $D = 1.0 \pm 0.1$.

TABLE II
MEASURED CHARACTERISTICS OF THE MIXER CORRELATOR AND MULTIPLIER CORRELATOR OVER THE 100–1000 MHz AND 90–520 MHz FREQUENCY RANGE, RESPECTIVELY

	Mixer correlator	Multiplier correlator
Noise bandwidth (MHz)	897	403
Dynamic range (dB) @ $\tau = 0.5$ s	46	48
Phase variations (mean) (deg)	2.7	1.0
Amplitude flatness (dB)	1.4	3.9
Degradation factor D	0.997	0.965
Input matching (dB)	< -19	< -17
Relative stability (dB) @ $\tau = 1$ s / 100 s	$-47 / -57$	$-55 / -55$

The measurement is very sensitive to systematic errors, but the rough value indicates that the degradation factor should be near the ideal value.

V. CONCLUSION

A continuum correlator based on a microwave nonlinear device, such as a mixer or a multiplier, is a simple and inexpensive way to detect wideband polarized signals. As component technology improves, the critical elements of such devices operate at wider bandwidths. The design of correlators described above requires only basic microwave measurements, which further simplifies the possible upgrade of the device.

Two different correlator topologies were studied in order to compare the basic characteristics and their influence on the resulting performance for applications in radio astronomy and airborne remote sensing.

The input band of the mixer correlator is very wide due to the simplicity of the active device. The simple design, on the other hand, limits the input power level, which somewhat reduces the dynamic range of the device. This should be kept in mind when the receiver is designed. The flat input reflection level allows the use of lossy match, which is a simple wide-band technique. The highest required input power levels can easily be achieved with standard class "A" RF amplifiers. The use of better temperature stabilization of the device would enhance the dynamic range of the correlator. The amplitude and phase response as well as the input match would enable the use of the mixer correlator at frequencies up to 1300 MHz. This would further improve the sensitivity about 15 %. The stability of the mixer correlator is good showing no degradation due to drift components at 30 s integration times.

The amplitude flatness of the mixer correlator is better than that of the multiplier correlator; on the other hand the multiplier correlator has flatter phase response. However, the measured parameters for both correlators were within the specified values. Both designs led to an almost ideal degradation factor, which indicates only a minimal decrease in the correlator channel sensitivity due to the correlator.

The multiplier correlator operates best at frequencies under 500 MHz. However, the increase in the amplitude and phase variations at higher frequencies is compensated by the broader

bandwidth; by taking the degradation factor D into consideration, the sensitivity improvement would be almost 20 % by applying a 100–700 MHz band instead of the 100–500 MHz band. The sensitivity improvement by using a 100–1000 MHz band would be almost 50 %. Above 700 MHz a wider-band matching should be applied due to high input reflections.

The sensitivity of a microwave receiver improves as the detected bandwidth becomes broader. Therefore, maximum bandwidth is pursued in many application of radio astronomy and remote sensing. A broadband and large dynamic range was obtained for both correlators in this study. The analog multiplier used for this study has very wide bandwidth for a commercially available component, but the current level of technology limits the use of the Gilbert cell multipliers to frequencies below 1 GHz. Balanced mixers provide generally wider bands than multipliers. Therefore, the bandwidth requirement being higher than 1 GHz, the use of mixers is endorsed. However, analog multipliers with noticeably broader bands can be expected to become available in the near future due to the recent advances in fast analog multiplier development [11]–[13]. Furthermore, the Gilbert Cell topology of the multiplier correlator provides good temperature stability; continuous calibration is not necessary, which is a major advantage, e.g., for airborne remote sensing applications. The stability could be further enhanced with the use of a biphaser shifter. Therefore, the use of a multiplier correlator that is based on Gilbert Cell topology is encouraged for applications that require high stability, given that the bandwidth requirements can be met. For many applications in radio astronomy and remote sensing, however, both mixer and multiplier approaches can meet the required bandwidth and stability requirements. In that case, also, all the other characteristics (e.g., dynamic range, degradation factor, linearity) of potential components should be carefully considered. According to our measurements, nearly ideal analog correlators can be designed with a wide variation of technical realizations. Only standard measurement equipment, available in almost any design facility, is needed to validate and compare the designs.

ACKNOWLEDGMENT

The authors would like to thank Prof. A. Räisänen, Radio Laboratory, Helsinki Univ. of Technology, for valuable comments during this work.

REFERENCES

- [1] S. Padin, "A wideband analog continuum correlator for radio astronomy," *IEEE Trans. Instrum. Meas.*, vol. 43, pp. 782–785, Dec. 1994.
- [2] N. R. Price, P. P. Kronberg, K. Iizuka, and A. P. Freundorfer, "Linear electro-optic effect applied to a radio astronomy correlator," *Radio Sci.*, vol. 31, no. 2, pp. 451–458, Mar.–Apr. 1996.
- [3] C. S. Ruf, "Constraints on the polarization purity of a Stokes microwave radiometer," *Radio Sci.*, vol. 33, no. 6, pp. 1617–1639, Nov.–Dec. 1998.

- [4] J. Lahtinen and M. Hallikainen, "Polarimetric radiometer for remote sensing," in *Proc. ESA Workshop Millim. Wave Technol. Applicat.: Antennas, Circuits Syst.*, Espoo, Finland, 1998, pp. 361–365.
- [5] M. Hallikainen, M. Kemppinen, J. Pihlflyckt, I. Mononen, T. Auer, K. Rautiainen, and J. Lahtinen, "HUTRAD: Airborne multifrequency microwave radiometer," in *Proc. ESA Workshop Millim. Wave Technol. Applicat.: Antennas, Circuits Syst.*, Espoo, Finland, 1998, pp. 115–120.
- [6] A. R. Thompson, J. M. Moran, and G. W. Swenson, Jr., *Interferometry and Synthesis in Radio Astronomy*. New York: Wiley, 1986, pp. 155–168.
- [7] M. E. Tiuri, "Radio astronomy receivers," *IEEE Trans. Antennas Propagat.*, vol. AP-12, pp. 931–938, Dec. 1964.
- [8] A. R. Thompson and L. R. D'Addario, "Frequency response of a synthesis array: Performance limitations and design tolerances," *Radio Sci.*, vol. 17, no. 2, pp. 357–369, Mar.–Apr. 1982.
- [9] R. Schieder, G. Rau, and B. Vowinkel, "Characterization and measurement of system stability," *Proc. SPIE Instrum. Submillim. Spectroscopy*, vol. 598, pp. 189–192, 1986.
- [10] D. W. Allan, "Statistics of atomic frequency standards," *Proc. IEEE*, vol. 54, pp. 221–230, Feb. 1966.
- [11] K. Osafune and Y. Yamauchi, "20-GHz 5 dB-gain analog multipliers with AlGaAs/GaAs HBT's," *IEEE Trans. Microwave Theory Tech.*, vol. 42, pp. 518–520, Mar. 1994.
- [12] Y. Imai, S. Kimura, Y. Umeda, and T. Enoki, "A DC to 38-GHz distributed analog multiplier using InP HEMT's," *IEEE Microwave Guided Wave Lett.*, vol. 4, pp. 399–401, Dec. 1994.
- [13] K. W. Kobayashi, R. M. Desrosiers, A. Gutierrez-Aitken, J. C. Cowles, B. Tang, L. T. Tran, T. R. Block, A. K. Oki, and D. C. Streit, "A DC-20-GHz InP HBT balanced analog multiplier for high-data-rate direct-digital modulation and fiber-optic receiver applications," *IEEE Trans. Microwave Theory Tech.*, vol. 48, pp. 194–202, Feb. 2000.



Olli Koistinen received the M.Sc. and Lic.Sc. degrees from the Helsinki University of Technology (HUT), Espoo, Finland, in 1990 and 1993, respectively.

He has worked in the field of low noise millimeter wave receivers with the Radio Laboratory, HUT, and with the Metsähovi Radio Observatory, HUT (1990–2000). He is currently with Nokia Corporation, Nokia Networks, and works as a part-time Research Scientist at the Metsähovi Radio Observatory, HUT.



Janne Lahtinen received the M.Sc. and Lic.Sc. degrees from the Helsinki University of Technology (HUT), Espoo, Finland, in 1996 and 2001, respectively.

He is currently a Research Scientist with the Laboratory of Space Technology, HUT, which he joined 1995. His research has focused on microwave radiometer systems, with special emphasis on polarimetric radiometers. He has authored and co-authored more than 20 publications in the area of microwave remote sensing.

Mr. Lahtinen served as a secretary of the Finnish National Committee of COSPAR from 1997 to 2002 and as a secretary of the Space Science Committee, appointed by Finnish Ministry of Education, from 1999 to 2000. He received the third place in the IEEE GRS-S Student Prize Paper Competition in 2000 and he won the Young Scientist Award of the National Convention on Radio Science in 2001.



Martti T. Hallikainen (F'93) received the M.Sc. degree in engineering and the Dir.Tech. degree from the Faculty of Electrical Engineering, Helsinki University of Technology (HUT), Espoo, Finland, in 1971 and 1980, respectively.

Since 1987, he has been Professor of Space Technology at the HUT, where his research interests include remote sensing and satellite technology. In 1988, he established the HUT Laboratory of Space Technology and serves as its Director. He was a Visiting Scientist from 1993 to 1994 at European

Union's Joint Research Centre, Institute for Remote Sensing Applications, Ispra, Italy. He was a Postdoctoral Fellow at the Remote Sensing Laboratory, University of Kansas, Lawrence, from 1981 to 1983, and was awarded an ASLA Fulbright Scholarship with the University of Texas, Austin, in 1974-1975.

Dr. Hallikainen served as President of IEEE Geoscience and Remote Sensing Society (IEEE GRSS) in 1996 and 1997, and as Vice President in 1994 and 1995. Since 1988, he has been a member of IEEE GRSS Administrative Committee and since 1999, he has served as IEEE GRSS Nominations Committee Chair. He was General Chairman of the IEEE IGARSS'91 Symposium and Guest Editor of the Special IGARSS'91 Issue of the IEEE TRANSACTIONS ON GEOSCIENCE AND REMOTE SENSING (TGARS). Since 1992, he has been Associate Editor of TGARS. He was a member of IEEE Periodicals Committee in 1997 and corresponding member of the IEEE New Technology Directions Committee from 1992 to 1995. He was Secretary General of the European Association of Remote Sensing Laboratories (EARSeL) from 1989 to 1993 and Chairman of the Organizing Committee for the EARSeL 1989 General Assembly and Symposium. He has been a member of EARSeL Council since 1985 and he was member of the Editorial Board of the EARSeL Advances in Remote Sensing from 1992 to 1993. He has been a member of the European Space Agency's (ESA) Earth Science Advisory Committee since 1998 and a member of ESA SMOS Scientific Advisory Group since 2000. He was a national delegate to the ESA Earth Observation Scientific and Technical Advisory Group (EOSTAG) from 1988 to 1994, and he has served in the same capacity on the ESA Earth Observation Data Operations Scientific and Technical Advisory Group (DOSTAG) since 1995. He was Thematic Coordinator of ESA EMAC-95 airborne campaign for Snow and Ice activities. He was a member of the ESA Multi-frequency Imaging Microwave Radiometer (MIMR) Expert Group from 1988 to 1994 and a member of the ESA MIMR Scientific Advisory Group from 1994 to 1996. He has been a member of the Advisory Committee for the European Microwave Signature Laboratory of the European Union's Joint Research Centre since 1992 and National Liaison of the International Space University since 1992. He served as Commission F Vice Chair of International Union of Radio Science (URSI) from 1999 to 2002. He was a member of the URSI Long Range Planning Committee from 1996 to 1999, he has been an official member of URSI Commission F (Wave Propagation and Remote Sensing) since 1988, he was a member of URSI Committee on Geosphere and Biosphere Program from 1989 to 1999, and he has been URSI representative to SCOR since 1999. He was Secretary of the Organizing Committee for the URSI Nordic Antenna Symposium in 1976 and he served as Secretary of the Finnish National Committee of URSI from 1975 to 1989. He was Vice Chairman of the URSI Finnish National Committee from 1990 to 1996 and he has served as Chairman since 1997. He has been Vice Chair of the Finnish National Committee of COSPAR since 2000. He is the recipient of three IEEE GRSS Awards: 1999 Distinguished Achievement Award, IGARSS'96 Interactive Paper Award, and 1994 Outstanding Service Award. He is the winner of the Microwave Prize for the best paper in the 1992 European Microwave Conference and he received the HUT Foundation Award for excellence in research in 1990. He and his research team received the 1989 National Research Project of the Year Award from Tekniikka & Talous (*Technology & Management Magazine*). He also received the 1984 Editorial Board Prize of Sähkö—Electricity in Finland.